DESIGN AND ANALYSIS OF A 3D PRINTED RC AIRCRAFT

Paul-Sebastian SUCIU
"Transilvania" University of Braşov, Romania (paul.suciu@student.unitbv.ro)

Sebastian-Marian ZAHARIA
"Transilvania" University of Braşov, Romania (zaharia_sebastian@unitbv.ro)
ORCID: 0000-0002-8636-5558

DOI: 10.19062/1842-9238.2023.21.1.2

Abstract: *3D printing of radio-controlled aircraft brings a major advantage, especially for prototype aircraft, as it can provide performance information in the shortest time and at the lowest cost. In this study, a model of a radio-controlled aircraft with high wing and tricycle landing gear was designed, aerodynamically analysed, simulated in FEA and manufactured by 3D printing. The aerodynamic performance showed a lift coefficient of 1.15 at a drag coefficient value of 0.10. From the FEA simulation, the wing structure was proven to withstand the stresses arising during the flight of the radio-controlled aircraft. It also demonstrated the feasibility of 3D printing in the case of radio-controlled aircraft prototypes, ready for the first flight tests.*

Keywords: *3D printing, radio-controlled aircraft, CFD analysis, finite elements analysis*

1. INTRODUCTION

There is a vast diversity of radio-controlled aircraft (or simple models) that can be produced by 3D printing, the deciding factor being the flight mission. In terms of design, there are small-scale, semi-scaled or prototype models. Small-scale and semi-scaled models are reproductions of existing aircraft, the only difference being the degree of accuracy; prototypes do not follow the design of an existing aircraft [1], but rather the development and testing of the innovative aircraft model [2].

Several types of radio-controlled aircraft that have been manufactured by 3D printing are presented below:

• Training aircraft are made for beginners to learn to fly. They have a conventional design, with the wing placed above the fuselage to ensure maximum stability. Training aircraft can be powered by electric motors or internal combustion motors. Their range is vast and represents a large subdivision of RC models [3].

• Sport aircraft can be designed as the next step after the pilot's becoming familiar with a training aircraft, but there is also the option of using them for the same purpose. Sport aircraft have a higher aerobatic capability than training aircraft. This is made possible by placing the wing at the middle or under the fuselage [4].

• The hydroplanes are a less popular choice because of the need for a landing site (preferably a lake). As with aerobatic aircraft, these types of RC models require a higher degree of experience, especially when it comes to landings [5].

• Warbird type of aircraft have always been a popular choice for RC models; the aesthetic design and good aerodynamic characteristics have made this type one of the most popular.

The term 'Warbird' refers to fighter aircraft from the time of the World War I and particularly the World War II. The P-51 Mustang, Spitfire and Corsair F4U are some classic examples. This range is not necessarily suitable for beginners, but there are 'Warbird' type models designed for this purpose [6].

• Aerobatic planes are specifically designed to perform aerobatics. This type of aircraft typically has oversized control surfaces and motor, and a mid-wing. This category is addressed to people with a certain degree of experience [7].

Based on the analysis of the current state of knowledge, the following aspects can be concluded [8-10]: 3D printing can be used to manufacture various aircraft prototypes in a relatively short time, without the need for a mould; additive technology has the potential to replace a multitude of current technologies; the most widely used material for 3D printing of models is polylactic acid (PLA), the wingspan of the aircraft varies between 900-16000 mm, the models have a relatively high mass, in the case of 3D printers intended for the general public, their accuracy is low.

2. RC MODEL DESIGN

Based on the analysis of the structural solutions, the design of a training aircraft was chosen with the following structural details: the wing has a rectangular shape and is placed above the fuselage; the fuselage is cylindrical; the shape of the horizontal empennage is trapezoidal; the empennages are arranged in a conventional configuration; the landing gear is of the tricycle type with tail wheel. The software system used for the wing design, and therefore for the design of the whole aircraft, was SolidWorks 2019. Next, the steps of the wing design are summarized: the airfoil (Clark Y) was inserted, the ribs were created (Fig. 1a), the ribs were cut for the lightening holes, the servo mount was set (Fig. 1b).

(a)

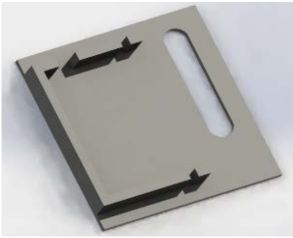

(b)

FIG. 1 Three-dimensional model of the RC aircraft wing: (a) wing rib structure, (b) servo mount.

The profile chosen for the horizontal (Fig. 2a) and vertical (Fig. 2b) empennage was NACA 0009. The ribs for the two empennages have been designed as for the wing.

(a)

(b)

FIG. 2 Three-dimensional model: (a) horizontal empennage, (b) vertical empennage.

In order to design the fuselage, planes and circular sections were created and then the assembly areas of the wing and motor mount were cut out (Fig. 3a). The 3D model of the radio-controlled aircraft prepared for 3D printing is shown in Fig. 3b. The 3D model (Fig. 3b) had the following dimensions: wingspan 900 mm, length 675 mm and height 180 mm.

(a) (b)

FIG. 3 RC aircraft design: (a) structure of the fuselage, (b) final model of the RC aircraft.

3. CFD ANALYSIS OF 3D PRINTED RC AIRCRAFT

The software system used for the CFD analysis of the radio-controlled aircraft was XFLR5 V6.48. In order to obtain the wing and aircraft curve polars, it is necessary to analyse in advance the profiles used (Clark Y and NACA 0009). For the wing analysis, the following input data were established: default speed of 13.8 m/s; the angles of attack for which this analysis is performed range from - 5° to 12°.

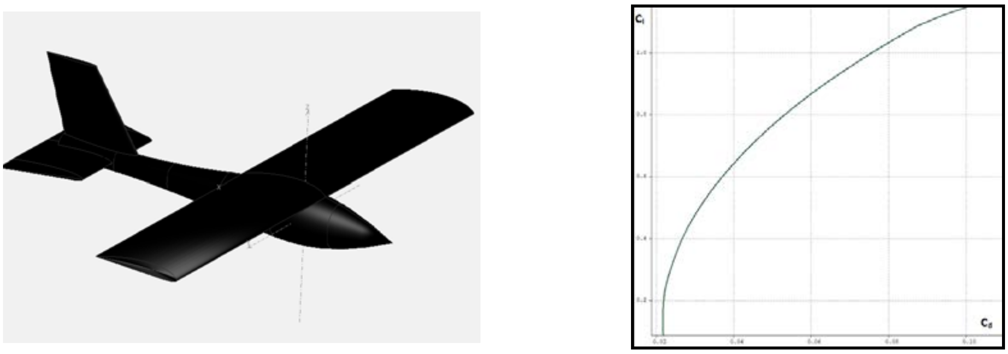

(a) (b)

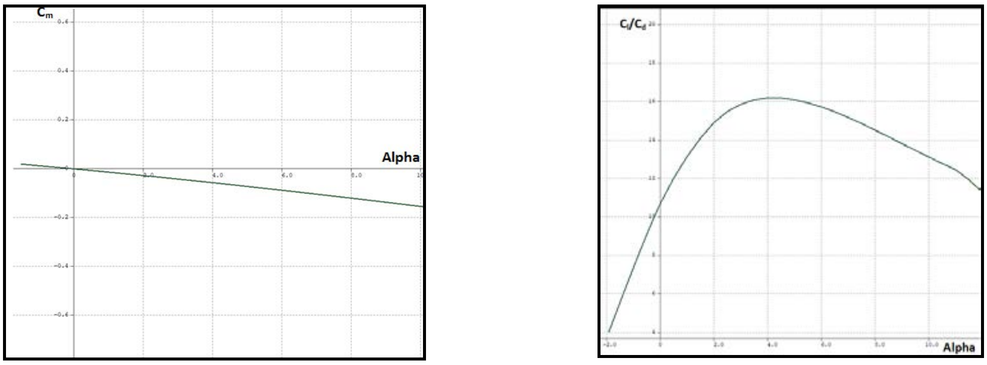

(c) (d)

FIG. 4 The preliminary aerodynamic analysis of the RC airplane: (a) 3d model of the aircraft, (b) variation of lift coefficient as function of drag coefficient, (c) variation of moment coefficient as function of the angle of attack, (d) variation of lift/drag ratio as function of the angle of attack.

After 3D modelling of the entire aircraft (Fig. 4a) the most important results of the aerodynamic analysis were determined: variation of lift coefficient as function of drag coefficient (Fig. 4b), variation of moment coefficient as function of angle of attack (Fig. 4c), variation of lift/drag ratio as function of angle of attack (Fig. 4d). The maximum value of the lift coefficient was 1.15 units for a value of drag equal to 0.103 units (Fig. 4b). To have a statically stable aircraft, the slope of the Cm- Alpha curve (α) must be negative. The smaller the slope value, the more stable the aircraft, so it can be seen in Fig. 4c that the slope value is negative. The lift/drag ratio of the aircraft increases with increasing the angle of attack. It reaches a maximum value of 16 units at 4° angle of attack. After exceeding this angle, the fineness decreases (Fig. 4d).

4. FINITE ELEMENT ANALYSIS OF THE 3D PRINTED RC WING

The finite element analysis of the strength structure is carried out for the wing semispan in the Ansys 2016 software system. The semispan was chosen to simplify the fixing method. The force applied for the wing stress was 29.43N, calculated as the product of the load factor (n=2), the aircraft mass (m=1 kg), the safety factor (SF=1.5) and the gravitational acceleration (9.81 m/s^2). Next, some important aspects were established: the material used for the model, in this case polylactic acid, was defined, the mashing of the model was performed with an element size of 3 mm, the wing was fixed in the embedding area and the force was uniformly applied over the entire surface of the shell (F=29.43N). The total displacements showed a maximum of 6.06 mm in the tip area of the wing (Fig. 5a). The maximum equivalent stresses (Fig. 5b) had values of 5.64 MPa near the embedment area of the wing to the fuselage. It can be concluded that the equivalent stress does not exceed the compressive strength of the PLA material. The maximum compressive strength of polylactic acid is 60.5 MPa, so the wing withstands the applied loadings.

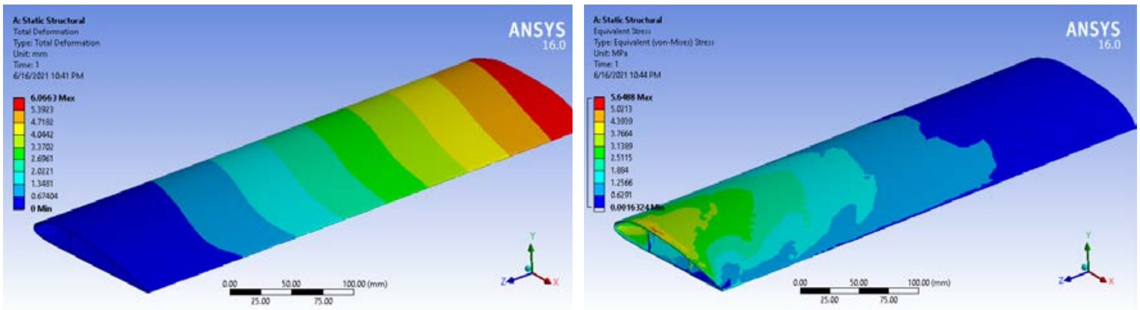

(a) (b)

FIG. 5 Finite element analysis: (a) total deformation, (b) equivalent stress.

5. MANUFACTURING THE RADIO-CONTROLLED AIRCRAFT PARTS USING 3D PRINTING

The 3D printer used to manufacture the radio-controlled aircraft parts was the Zortrax M200 Plus. The software system used to 3D print the aircraft parts was Z-Suite. Among the most important parameters we can list: the thickness of the deposition layer was 0.14 mm and the infill density was 50%, the printing temperature was 200 °C, the temperature of the bed plate was 30°C, and the material was polylactic acid (PLA). Figure 6a shows some of the parts prepared for 3D printing in the Z-Suite software system and Fig. 6b shows the 3D printed parts.

Also, in Fig. 6c some sections of the fuselage were prepared for 3D printing and in Fig. 6d these parts can be seen after they were printed. The total printing time for all the parts of the aircraft was 171 hours and the amount of PLA filament required was 1270 grams.

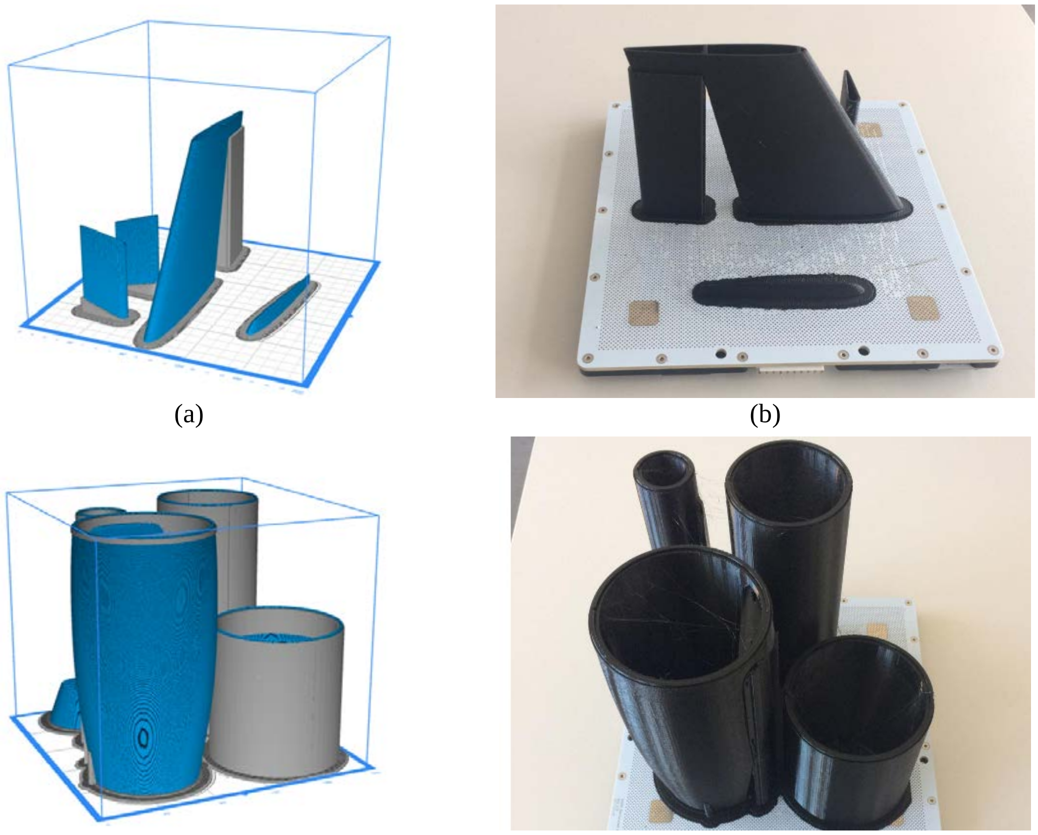

(a) (b) (c) (d)

FIG. 6 Steps in the 3D printing process: (a) preparation for manufacturing of the vertical fuselage, (b) 3D printed vertical fuselage, (c) preparation for manufacturing of the fuselage sections, (d) 3D printed fuselage sections.

6. ASSEMBLY AND GROUND TESTING OF THE 3D PRINTED RC WING

To assemble the aircraft, a series of steps were carried out: the support material from the 3D-printed parts was removed, the rear sub-assembly consisting of the empennages and the last fuselage section was glued (Fig. 7a); the parts of the aircraft were sanded with sandpaper, the wing sections were glued (Fig. 7b) and two-component adhesive was used to make all the joints; before gluing the wing tips, the servo extensions were inserted; for aesthetic reasons, the radio-controlled aircraft was painted; the next step involved attaching the control surfaces using a fibreglass adhesive strip; the servo-mechanisms were assembled and coupled to the control rods.

Regarding the manufacturing and assembly of the landing gear (Fig. 7c), it was decided to use stainless steel rods (D=2 mm). The landing gear was arc welded at the wheels. The mounting of the rear landing gear was done by means of pocket hole screws. The next step was the assembly of the electrical parts consisting of the regulator, transmitter, battery and propeller. The parts are fixed inside the fuselage by means of an adhesive strip with Velcro, except for the motor, which is fixed to the motor mount with screws.

The electrical parts used were brushless outrunner motor SUNNYSKY X2212, the speed controller used is brushless Fly Pro - 40A, LiPo battery 2700 mAh, the transmitter and receiver used to fly the aircraft are the Radiolink AT9S. The final design of the aircraft is shown in Fig. 7d.

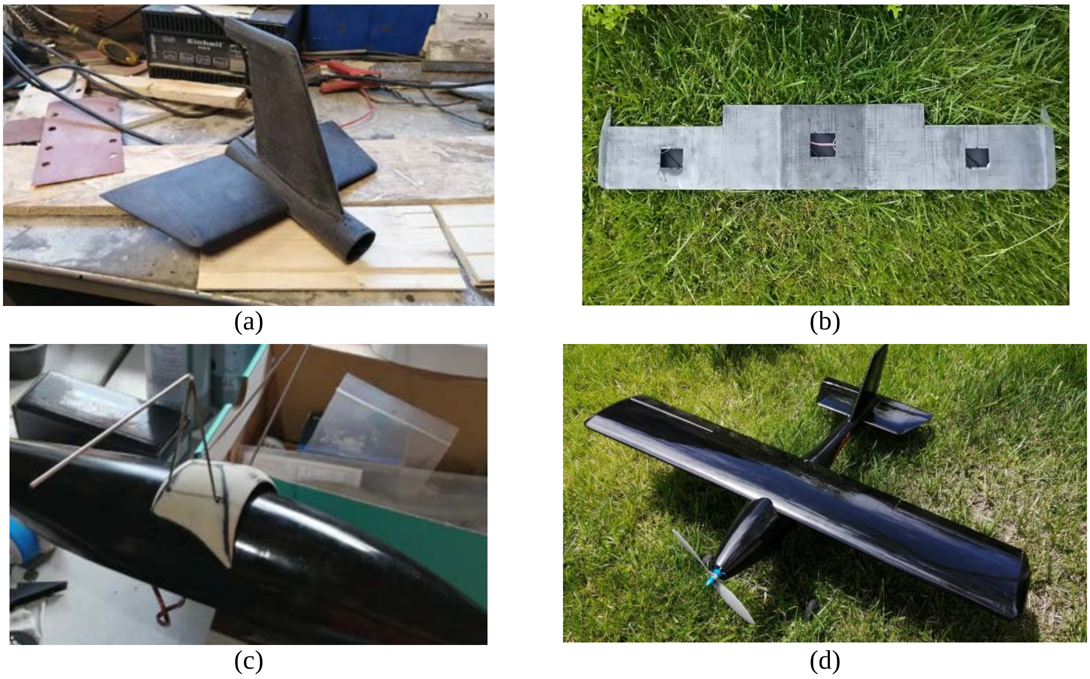

(a) (b) (c) (d)

FIG. 7 Stages in the assembly process: (a) gluing the rear subassembly, (b) assembling and gluing the wing, (c) manufacturing the landing gear, (d) the 3D printed radio-controlled aircraft.

In the last stage, ground testing of the control surfaces was carried out as follows: rudder deflection (Fig. 8a), elevator deflection (Fig. 8b), aileron deflection and the correct operation of the electric motor was also checked (Fig. 8c).

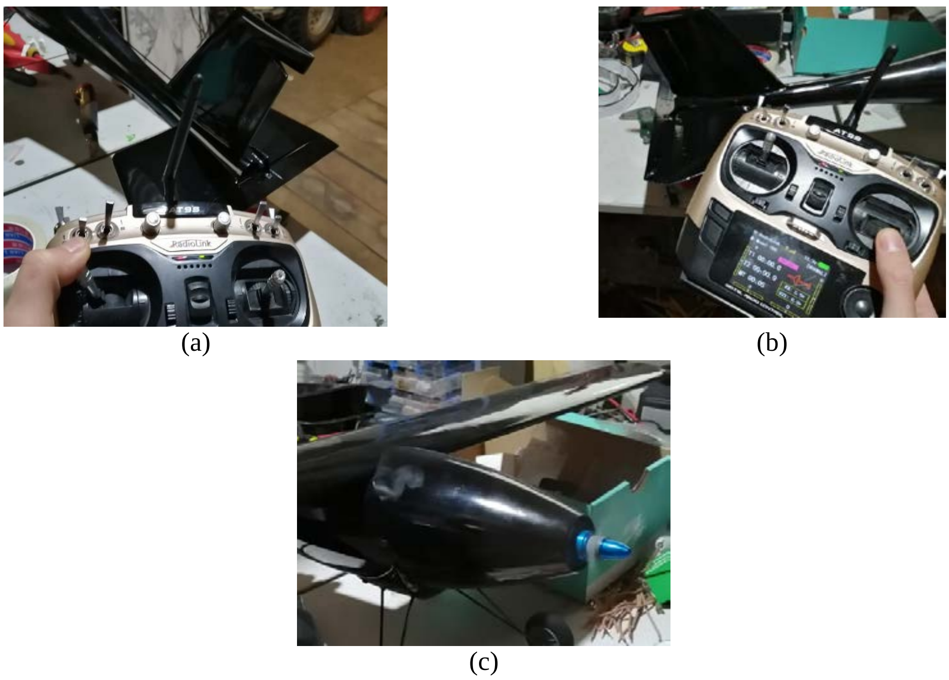

(a) (b) (c)

FIG. 8 Ground testing: (a) motor testing, (b) rudder movement, (c) elevator deflection.

CONCLUSIONS

The current state of knowledge about aircraft shows the simplicity of additive processes, in that no moulds are required to make the models. Another advantage worth mentioning in this context is the reduced manufacturing time. The designed and 3D printed aircraft has a mass of about 1800 g and a range of 6-10 minutes, depending on the type of flight. From the CFD analysis the polar curves of the most important aerodynamic coefficients (lift coefficient, drag coefficient and momentum coefficient) were determined and plotted. From the FEA simulation, the maximum compressive strength of polylactic acid is much higher compared to the equivalent stress obtained from the finite element analysis of the wing. The 3D printing of the radio-controlled aircraft parts from PLA filament was carried out without any problems and the manufacturing time was 171 hours.

The main goals of the assembly technology were to manufacture a visually aesthetic and structurally strong aircraft. In the final phase, ground tests were carried out to check the operation of the control surfaces and the electric motor. In conclusion, it is possible to manufacture aircraft using 3D printing in a relatively short time and without the need for moulds, at low cost, using an affordable additive process.

REFERENCES

[1] A. Olejnik, S. Kachel, R. Rogólski and J. Milczarczyk, The concept and methodical assumptions for the development of dynamically scaled aircraft model (passenger aircraft), MATEC Web of Conferences, vol. 304, 2019;

[2] K. Patel, Y. Parmar, V. Parmar, H. Mistry and M. Tandel, A Review Article on Design and Development of Radio-Controlled Airplane, International Journal of Advances in Engineering and Management, vol. 2, no. 7, pp. 41-46, 2008, 2019;

[3] *** 3D LabPrint, QTRAINER aircraft. Available at https://3dlabprint.com/shop/qtrainer/, accessed on 10 May 2023;

[4] D. A. Popica and S. M. Zaharia, Design, aerodynamic analysis and additive manufacturing of a radio-controlled airplane, Journal of Industrial Design and Engineering Graphics, vol. 18, no.1, pp.39-44, 2023;

[5] *** RC3DPRINT, Grumman Mallard aircraft. Available at https://www.rc3dprint.com/mallard, accessed on 12 May 2023;

[6] *** 3D LabPrint, P51-D MUSTANG aircraft. Available at https://3dlabprint.com/shop/p51-d-mustang/, accessed on 11 May 2023;

[7] *** PLANEPRINT, SHARD aircraft. Available at https://www.planeprint.com/shard, accessed on 11 May 2023;

[8] I. S. Pascariu and S. M. Zaharia, Design and testing of an unmanned aerial vehicle manufactured by fused deposition modeling, *Journal of Aerospace Engineering*, vol. 33, no. 4, 2020;

[9] I. Skawiński and T. Goetzendorf-Grabowski. 2019. “FDM 3D printing method utility assessment in small RC aircraft design.” Aircraft Eng. Aerosp. Technol. 91 (6): 865–872;

[10] M., Hassanalian and A. Abdelkefi, Classifications, applications, and design challenges of drones: A review, *Progress in Aerospace Sciences*, vol. 91, pp. 99-131, 2017.